Raman Heterodyne Detection of Nuclear Magnetic Resonance

J. Mlynek,[a] N. C. Wong, R. G. DeVoe, E. S. Kintzer, and R. G. Brewer
IBM Research Laboratory, San Jose, California 95193, and Department of Applied Physics, Stanford University, Stanford, California 94305

(Received 7 December 1982)

An optical heterodyne technique based on the coherent Raman effect is demonstrated for detecting nuclear magnetic resonances (NMR) and coherent spin transients in normal and optically excited impurity-ion solids at low temperature. Initial measurements on Pr^{3+}:LaF_3 provide the first spin-echo studies of an electronically excited state, and cw resonances yield NMR line centers and shapes with kilohertz precision.

PACS numbers: 76.70.-r, 76.60.-k, 78.30.-j

This Letter reports a new way of detecting nuclear magnetic resonance in solids with a coherent optical and radio-frequency induced Raman effect. The technique, which employs heterodyne detection, is capable of monitoring coherent spin transients or nuclear resonances under cw conditions, in both ground and excited electronic states. As a result of the high sensitivity and precision, dilute systems in the gas phase or solid can now be examined which are inaccessible by conventional NMR. Furthermore, the method surpasses previous optical-rf measurements, especially for excited electronic states which have remained elusive. We illustrate the versatility of the method in a dilute rare-earth impurity-ion crystal, Pr^{3+}:LaF_3, where Pr^{3+} spin echoes of nuclear quadrupole transitions are detected not only in the $^3H_4$ ground electronic state but also for the first time in the $^1D_2$ excited state, thus allowing a critical test of current line broadening theory. From the cw spectrum, the Pr^{3+} hyperfine splittings in these electronic states, as well as the magnetically broadened inhomogeneous line shapes and widths, are determined with kilohertz precision, about a fivefold improvement over earlier measurements.

In Fig. 1(b), the Pr^{3+} ($I=\frac{5}{2}$) electron-hyperfine energy-level diagram reveals the basic stimulated Raman process where two coherent fields, one at the optical frequency Ω (solid arrow) and the other at the rf frequency ω (squiggle arrow), drive two coupled transitions resonantly. The electric-dipole-allowed optical transition $^3H_4(I_z=\frac{5}{2}) \rightarrow {}^1D_2(I_z=\frac{5}{2})$ and the magnetic-dipole-allowed quadrupole transition $^3H_4(I_z=\frac{3}{2} \leftrightarrow \frac{5}{2})$ combine in a two-photon process to generate a coherent optical field at the sum frequency $\Omega' = \Omega + \omega$ (dashed arrow). This transition is also electric dipole allowed because the $^1D_2$ hyperfine states are mixed by the nuclear quadrupole interaction. In addition, a Stokes field at the difference frequency $\Omega - \omega$ (not shown), due to a second resonant packet, accompanies the above anti-Stokes field.

In Fig. 2, we see that when the two optical fields (Ω and Ω') strike a photodetector a heterodyne beat signal of frequency $\omega = |\Omega - \Omega'|$ appears, a feature which enhances detection sensitivity. The heterodyne process occurs automatically as part of the basic interaction and thus is closely related to Stark or laser frequency-switching experiments[1] which produce in two-photon processes coherent Raman beats[2] or heterodyne beats in one-photon coherent transients.[1]

The present case differs from earlier studies of the stimulated Raman effect[3] where two optical

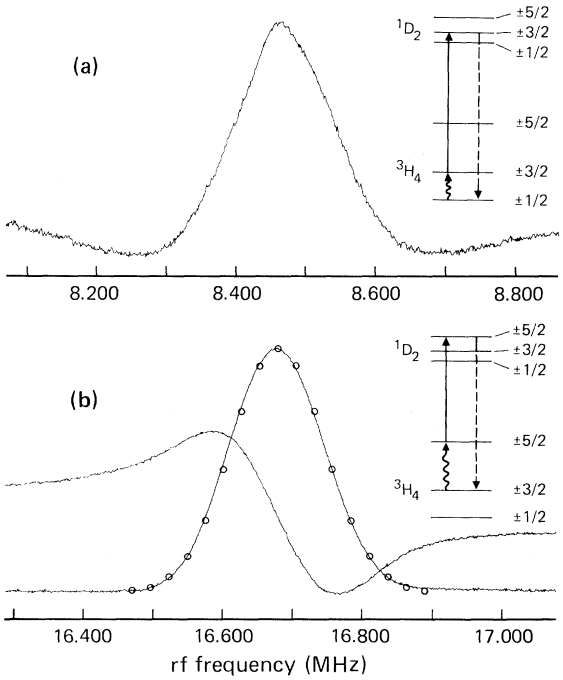

FIG. 1. Raman heterodyne NMR signals of the Pr^{3+}:LaF_3 $^3H_4$ ground-state spin transitions (a) $I_z=\frac{1}{2} \leftrightarrow \frac{3}{2}$ in absorption and (b) $\frac{3}{2} \leftrightarrow \frac{5}{2}$ in absorption and dispersion for $H_0 \sim 0$ G.

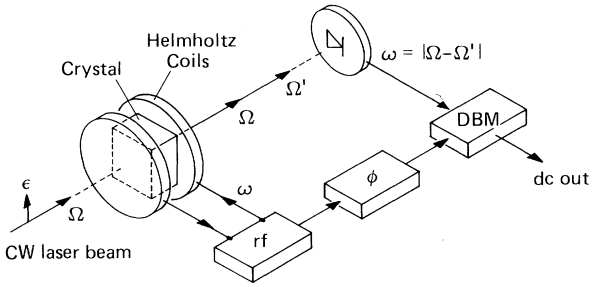

FIG. 2. Schematic of the experimental arrangement for Raman heterodyne detection of cw or pulsed NMR.

fields drive two coupled electric dipole transitions and the remaining third transition is radiatively inactive or is not monitored. Here, all three fields appear corresponding to the three possible transitions, a three-wave mixing effect. It also differs in that both electric and magnetic dipole transition are employed, and it is for this reason that NMR can be observed readily for the first time in a stimulated Raman process, under either cw or pulsed conditions. Note also that the technique can be generalized to any three-level system where all three transitions are active, allowing detection of NMR, ESR, or even infrared transitions.

Our work thus extends previous coherent techniques as in optical-pumping double resonance,[4] coherent Raman beats,[2] photon-echo modulation and nuclear double resonance,[5] and Raman echoes,[6] or those methods which rely on incoherent detection using optical spontaneous emission, for example, in rf-optical double-resonance experiments[7,8] or in enhanced and saturated absorption.[9] However, the present precision and sensitivity greatly surpass these techniques.

To predict the characteristics of the Raman heterodyne beat signal, we have performed a steady-state perturbation calculation for an inhomogeneously broadened three-level atom where the rf magnetic field drives the $1 \leftrightarrow 2$ transition and the laser field drives packets corresponding to the $1 \leftrightarrow 3$ and $2 \leftrightarrow 3$ transitions. This action generates coherent Stokes and anti-Stokes fields which in lowest order yield a heterodyne beat signal of the form

$$|E|_{\text{beat}}^2 = -a\chi\chi_1\chi_2(\rho_{22}^0 - \rho_{11}^0)\exp[-(\Delta/\sigma_\alpha)^2]\left[\cos\omega t\ \mathrm{Im}w\left(\frac{\Delta_{21}+i\gamma_{21}}{\sigma_\beta}\right) - \sin\omega t\ \mathrm{Re}w\left(\frac{\Delta_{21}+i\gamma_{21}}{\sigma_\beta}\right)\right], \quad (1)$$

where $a = \pi^2 kNL\hbar/\sigma_\alpha\sigma_\beta$, $\vec{k}$ being the optical propagation vector, N the atomic number density, and L the atomic optical path length. The function[10] $w(z) = (i/\pi)\int_{-\infty}^{\infty}\exp(-t^2)dt/(z-t)$ represents a convolution of an inhomogeneous Gaussian and a Lorentzian line shape, with σ_α the strain-broadened Gaussian linewidth for the optical transition, σ_β the Gaussian linewidth of the rf transition arising from static local magnetic fields, γ_{21} the homogeneous linewidth of the spin transition, $\Delta = \Omega - \omega_{31}$ the optical tuning parameter, and $\Delta_{21} = \omega - \omega_{21}$ the rf tuning parameter. The Rabi frequencies are $\chi = \mu_{12}H_1/\hbar$, $\chi_1 = \mu_{13}E_1/\hbar$, and $\chi_2 = \mu_{23}E_1/\hbar$ where μ_{ij} is the transition matrix element. Thus, the beat signal scales as the product of the rf magnetic field amplitude H_1 and the laser intensity E_1^2 where the two-photon process requires the product H_1E_1 and the heterodyne beat introduces an additional E_1 factor. To this order of approximation, the signal varies as the unperturbed population difference $(\rho_{22}^0 - \rho_{11}^0)$.

The beat Eq. (1) displays in- and out-of-phase components of the beat frequency ω and a Gaussian rf line shape, as in Fig. 1(b), when $\gamma_{21}/\sigma_\beta \ll 1$. When the laser frequency is tuned far off resonance, (1) predicts that the heterodyne beat vanishes even though the Stokes and anti-Stokes sidebands can remain strong. Physically, the optically resonant case corresponds to the Stokes and anti-Stokes sidebands being of the same phase (amplitude modulation) and thus add, whereas in the nonresonant case the two sidebands are of opposite phase (frequency modulation) and cancel. This suggests that the nonresonant Raman detection of NMR should be possible with FM detection.

The experimental configuration of Fig. 2 can be used for both cw and pulsed NMR experiments. The cw beam of a Coherent model 599 dye laser oscillating in the locked mode (linewidth 4 MHz peak to peak) at 5925 Å excites the Pr^{3+} $^3H_4 \rightarrow {}^1D_2$ transition by propagating along the c axis of a 0.1-at.% Pr^{3+}:LaF_3 crystal ($3.5\times3.5\times2$ mm^3) with a beam diameter of ~ 100 μm and power in the range 3 to 50 mW. Population loss by optical pumping is circumvented by laser frequency sweeping (sweep rate 400 MHz/0.5 sec) within the 5-GHz optical inhomogeneous line shape. Radio-frequency fields up to 30 G and in the range $\omega/2\pi = 3$ to 17 MHz are applied by a pair of small Helmholtz coils surrounding the crystal, as in Fig. 2, where both are immersed in a liquid-helium cryostat at 1.6 K. The coherently generated Stokes and anti-Stokes fields result in a hetero-

dyne beat signal of frequency $\omega = |\Omega - \Omega'|$ that is detected with a p-i-n diode and demodulated in a double-balanced mixer to yield absorption or dispersion line shapes, Fig. 1(b), according to the rf phase setting φ. Since the signals are large, video detection is feasible, and furthermore the noise level is *shot-noise limited* because the heterodyne detection process, unlike previous optical-rf methods, selects a frequency window where the laser noise is $10^8\times$ lower than the dc level.

Most of the features predicted by Eq. (1) are verified for the $^3H_4$ and $^1D_2$ quadrupole transitions. Consider first the 16.7-MHz transition of Fig. 1(b) where (1) the $H_1E_1^2$ field dependence is obeyed in the region of negligible power broadening, (2) the predicted (open circles) and observed (solid line) line shapes are essentially Gaussian, and (3) both absorptive and dispersive line shapes appear. The three-level model does not include, however, the effects of optical pumping and laser-frequency sweeping which dramatically increase the Pr^{3+} population difference $(\rho_{22}-\rho_{11})$ above the unperturbed value of Eq. (1) and improve the signal strength. In contrast, the line shape of Fig. 1(a) is not strictly Gaussian largely because of the appearance of a symmetrical pair of lobes in the wings of the line. This curious effect seems to depend in a complicated way on the optical pumping cycle, the rf sweep rate (range 1 MHz /10 msec to 1 MHz/60 sec) and whether one or two hyperfine transitions are excited in the same sweep.

Table I summarizes the Pr^{3+} quadrupole splittings and amplitude linewidths observed in the earth's magnetic field. These values are uncertain by at most a few kilohertz and thus reduce the error in previous measurements[5,7-9] by a factor of 5 or more. The $^1D_2$ linewidths compare favorably with Whittaker and co-workers[5] (60 ± 20 kHz full width at half maximum) and are significantly smaller than that of Erickson (200 ± 50 kHz)[9] which is limited by laser frequency stability. The $^3H_4$ values of Erickson[7] (180 ± 10 kHz) and that of Shelby, Yannoni, and Macfarlane[8] (230 kHz) appear to be power broadened. We find that the Table I linewidths decrease by ~30% when a dc field $H_0 > 50$ G is applied, bringing them into closer agreement with our $^3H_4$ Monte Carlo (82 kHz) and second-moment (84.5 kHz) calculations.[11] From the splittings and numerical eigenenergy solutions of the Pr^{3+} quadrupole Hamiltonian $\mathcal{H}_Q = D[I_z^2 - I(I+1)/3] + E(I_x^2 - I_y^2)$, we obtain for the $^3H_4$ state $D = 4.1795 \pm 0.0013$ MHz and $E = 0.154 \pm 0.004$ MHz ($\eta = 0.111 \pm 0.003$), while for $^1D_2$, $D = 1.2921 \pm 0.0009$ MHz and $E = 0.305 \pm 0.001$ MHz ($\eta = 0.708 \pm 0.002$).

We also have detected two-pulse spin echoes, as well as nutation and free-induction decay, in each of the four quadrupole transitions. Figure 3 shows spin echoes for the $^3H_4$ $(\frac{3}{2} \leftrightarrow \frac{5}{2})$ transition in a dc magnetic field $H_0 \sim 0$ G and for the $^1D_2$ $(\frac{3}{2} \leftrightarrow \frac{5}{2})$ line in a field $H_0 \sim 50$ G that enhances the signal ~ 10× and produces interferences among the Zeeman split lines in the free-induction decay following the initial two pulses and in the echo. *The $^1D_2$ excited-state spin echoes are the first observations of this kind.* For a field H_0 parallel to the crystal a axis, the homogeneous linewidths $(1/\pi T_2)$, full width at half maximum, derived from the spin-echo dephasing times T_2 are 21 ± 2 kHz for the $^3H_4$ $(\frac{3}{2} \leftrightarrow \frac{5}{2})$ line ($H_0 \sim 0$ G) and 15 ± 2 and

TABLE I. Raman-detected quadrupole splittings (ν) and linewidths ($\nu_{1/2}$, full width at half maximum) for the lowest Stark-split states of $^3H_4$ (ground state) and $^1D_2$ of Pr^{3+}(0.1 at.%):LaF_3 in the earth's magnetic field.

$I_z \leftrightarrow I_z$	ν (MHz)	$\nu_{1/2}$ (kHz)
$^3H_4$ (1/2 ↔ 3/2)	8.470 ± 0.005	159 ± 5
$^3H_4$ (3/2 ↔ 5/2)	16.677 ± 0.003	160.5 ± 1
$^3H_4$ (1/2 ↔ 5/2)	25.150 ± 0.003	259 ± 8
$^1D_2$ (1/2 ↔ 3/2)	3.724 ± 0.006	46.5 ± 1
$^1D_2$ (3/2 ↔ 5/2)	4.783 ± 0.001	45.3 ± 2.6

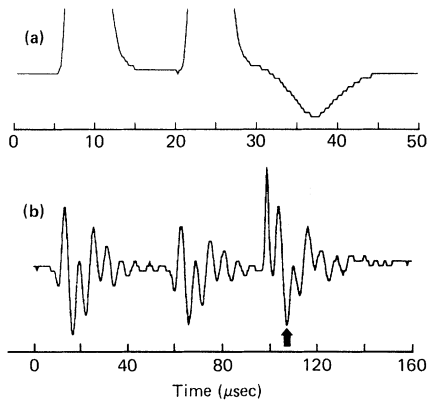

FIG. 3. Computer plot of Raman heterodyne detection of spin echoes for (a) the $^3H_4(\frac{3}{2} \leftrightarrow \frac{5}{2})$ spin transition where $H_0 \simeq 0$ G, $H_1 = 12$ G, the pulsed delay time $\tau = 15$ μsec, and the rf pulse widths are 1.8 and 3.0 μsec, and (b) the $^1D_2$ $(\frac{3}{2} \leftrightarrow \frac{5}{2})$ spin transition where $H_0 = 43$ G, $H_1 = 23$ G, $\tau = 50$ μsec, and the rf pulse widths are 3 and 4 μsec. In (b), the echo envelope is amplified ~ 10× and an arrow marks its center.

20 ± 2 kHz for the $^1D_2$ ($\frac{3}{2} \rightarrow \frac{5}{2}$) and ($\frac{1}{2} \rightarrow \frac{3}{2}$) lines ($H_0 > 30$ G). By comparison, rf-optical double resonance gives 19 kHz for the 16.7 MHz transition[8] and photon echo measurements[12] for $^3H_4 \rightarrow {}^1D_2$ yield 14 kHz. Furthermore, we can conclude using Table I that the magnetic homogeneous and inhomogeneous widths are comparable in the $^1D_2$ state whereas the inhomogeneous width dominates in the $^3H_4$ state. Very crudely, the excited and ground-state inhomogeneous linewidths scale as γ_z. However, to understand these comparisons more fully and to relate them in a self-consistent way, we plan to extend our earlier Monte Carlo line broadening theory.[11]

This brief article touches but a few examples. It is clear, however, that the full range of cw and pulsed NMR experiments can now be explored with equal facility in normal and optically excited low-temperature impurity-ion solids. In addition to Pr^{3+}:LaF_3, similar measurements have been conducted on Pr^{3+}:$YAlO_3$ and atomic gases.[13]

We are indebted to D. Horne and K. L. Foster for technical aid. One of us (N.C.W.) acknowledges support of a Hertz Foundation Graduate Fellowship. This work was supported in part by the U. S. Office of Naval Research.

---

[a]On leave from the Institut für Angewandte Physik, Universität Hannover, Hannover, West Germany.

[1]R. G. Brewer and R. L. Shoemaker, Phys. Rev. Lett. 27, 631 (1971); R. G. Brewer and A. Z. Genack, Phys. Rev. Lett. 36, 959 (1976).

[2]R. L. Shoemaker and R. G. Brewer, Phys. Rev. Lett. 28, 1430 (1972); R. G. Brewer and E. L. Hahn, Phys. Rev. A 8, 464 (1973).

[3]M. D. Levenson, *Introduction to Nonlinear Laser Spectroscopy* (Academic, New York, 1982), p. 17, and references therein.

[4]B. S. Mathur, H. Tang, R. Bulos, and W. Happer, Phys. Rev. Lett. 21, 1035 (1968).

[5]K. Chiang, E. A. Whittaker, and S R. Hartmann, Phys. Rev. B 23, 6142 (1981); E. A. Whittaker and S. R. Hartmann, Phys. Rev. B 26, 3617 (1982).

[6]S. R. Hartmann, IEEE J. Quantum Electron. 4, 802 (1968); P. Hu, S. Geschwind and T.M. Jedju, Phys. Rev. Lett. 37, 1357 (1976).

[7]L. E. Erickson, Opt. Commun. 21, 147 (1977); K. K. Sharma and L. E. Erickson, Phys. Rev. Lett. 45, 294 (1980).

[8]R. M. Shelby, C. S. Yannoni, and R. M. Macfarlane, Phys. Rev. Lett. 41, 1739 (1978).

[9]L. E. Erickson, Phys. Rev. B 16, 4731 (1977).

[10]*Handbook of Mathematical Functions*, edited by M. Abramowitz and I. Stegun (U.S. GPO, Washington, D.C., 1964), p. 297; R. G. DeVoe and R. G. Brewer, Phys. Rev. A 20, 2449 (1979).

[11]R. G. DeVoe, A. Wokaun, S. C. Rand, and R. G. Brewer, Phys. Rev. B 23, 3125 (1981).

[12]R. M. Macfarlane, R. M. Shelby, and R. L. Shoemaker, Phys. Rev. Lett. 43, 1726 (1979).

[13]J. Mlynek, to be published.